Pleckstrin Homology-Phospholipase C-δ 1 Interaction with Phosphatidylinositol 4,5-Bisphosphate Containing Supported Lipid Bilayers Monitored in Situ with Dual Polarization Interfer...

ARTICLE *in* ANALYTICAL CHEMISTRY · AUGUST 2011

Impact Factor: 5.64 · DOI: 10.1021/ac2009178 · Source: PubMed

4 AUTHORS:

Martina K Baumann
ETH Zurich Foundation
8 PUBLICATIONS **51** CITATIONS
SEE PROFILE

Marcus Jack Swann
Swann Scientific Consulting Ltd.
73 PUBLICATIONS **1,641** CITATIONS
SEE PROFILE

Marcus Textor
ETH Zurich
333 PUBLICATIONS **14,033** CITATIONS
SEE PROFILE

Erik Reimhult
University of Natural Resources and Life Scie...
93 PUBLICATIONS **2,985** CITATIONS
SEE PROFILE

analytical chemistry

ARTICLE

pubs.acs.org/ac

Pleckstrin Homology-Phospholipase C-δ_1 Interaction with Phosphatidylinositol 4,5-Bisphosphate Containing Supported Lipid Bilayers Monitored *in Situ* with Dual Polarization Interferometry

Martina K. Baumann,[†] Marcus J. Swann,[‡] Marcus Textor,[†] and Erik Reimhult*[,†,§]

[†]Department of Materials, Laboratory for Surface Science and Technology (LSST), ETH Zurich, Wolfgang-Pauli-Strasse 10, CH-8093 Zurich, Switzerland

[‡]Farfield Group, Farfield House, Southmere Court, Electra Way, Crewe Business Park, Crewe CW1 6GU, United Kingdom

[§]Department of Nanobiotechnology, University of Natural Resources and Life Sciences Vienna, Muthgasse 11, A-1190 Vienna, Austria

Supporting Information

ABSTRACT: We have determined the kinetics and affinity of binding of PH-PLCδ_1 to the PIP_2 headgroup lipids using an optical surface-sensitive technique in a time-resolved manner. The use of dual polarization interferometry to probe supported lipid bilayers (SLBs) of different compositions allowed determination of accurate affinity constants and a layer structure of the peptide binding to the model membrane platform. In addition, the platform enabled us to monitor the detailed adsorption kinetics characterized by a strong initial electrostatic attraction of the peptide to the SLB surface followed by rearrangement and loss of possibly clustered peptides upon specific binding to the phosphoinositide headgroup. These kinetics differed substantially from adsorption kinetics for nonspecific binding to similarly charged control SLBs.

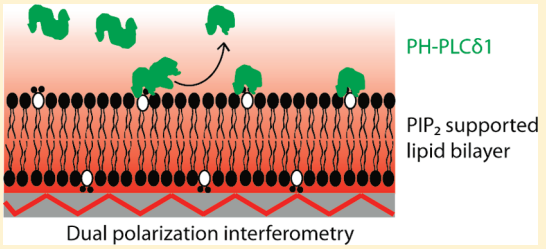

The interaction of some cytosolic proteins and cytosolic domains of membrane proteins is mediated by the headgroup of phosphoinositides. It has been discovered that such proteins only interact with a particular phosphorylation pattern but do not interact with phosphoinositides in general.[1] Different affinities for one or the other phosphorylation pattern is thus a likely factor to fine-tune and control specific signaling cascades. Phosphatidylinositol 4,5-bisphosphate (PIP_2) is the most abundant phosphoinositide in mammalian cells. It is mainly located at the cytosolic side of the plasma membrane. PIP_2 mediates a variety of cellular processes and serves as a substrate for phospholipase C (PLC) to generate the second messenger diacylglycerol (DAG, effector of protein kinase C) and inositol trisphosphate (IP_3, effector of Ca^{2+} signaling). PIP_2 also participates in several signaling pathways,[2] for which its control over diverse processes is suspected to be given not only by enzymatic regulation but also by regulation of the spatial distribution of PIP_2.[3] Thus, control over the lipid composition in the membrane as well as over the "cytosolic" environment is needed to capture the interactions between proteins and lipids to an extent that allows us to understand the details of regulatory pathways. Measuring specific affinities and kinetics of these events on *in vitro* cell systems is limited by the complexity and dynamics of cell membranes, where concentration and distribution of membrane species, including potential interaction partners, fluctuate continuously and greatly. Supported lipid bilayers (SLBs) for which a fixed lipid composition can be chosen to mimic the desired membrane features (e.g., surface charge, lipid head groups, acyl chain length and saturation) provide an attractive alternative to real cell systems in this respect. SLBs are also ideally suited to be combined with biosensor techniques for which interacting proteins can be applied in a controlled way and with quantitative, highly sensitive and, if desired, label-free readout of binding kinetics.

The pleckstrin homology domain (PH domain) was first described by Haslam et al. and named after the hematopoietic protein pleckstrin where this domain was first discovered.[4] This 100−120 residue homology sequence has since then been discovered in many proteins involved in signaling, cytoskeletal organization, and other processes.[5] A total of 13 different PH domains have been identified by NMR and X-ray crystallography.[6] These structures all have a common characteristic core β-sandwich fold and share more of a structural homology than a sequence homology (the sequence homology is often only 10−30%).[7] All proteins which carry a PH domain have a functional requirement for membrane association.[8] PH domains interact through electrostatic interactions mediated by basic amino acids in the three variable loops between the β sheets. The three variable loops form a positively charged surface which contains the phosphoinositide binding site in the center. Most of

Received: April 9, 2011
Accepted: July 5, 2011
Published: July 05, 2011

the PH domains exhibit weak specificity for their ligands. However, certain PH domain binding sites are well-defined and allow for specific and strong ligand binding, as for example, the pleckstrin homology domain of phospholipase C-δ_1 (PH-PLCδ_1) for PIP_2 and its free headgroup Ins(1,3,5)P_3.[8,9]

In this work, we present an *in vitro* platform using PIP_2 containing SLBs[10] in combination with a highly surface sensitive technique to study the interaction between lipids and protein domains in a quantitative manner as well as real time observation of the kinetics of the interaction. Dual polarization interferometry (DPI) allows for detection of conformational changes and binding events on the SLB surface.[11] To demonstrate the potential of this *in vitro* platform, we investigate the interaction of PH-PLCδ_1 with PIP_2 in SLBs of different composition. An analysis of the detailed adsorption kinetics revealed a multifaceted adsorption behavior including conformational rearrangements of the membrane−peptide complex, which could not have been measured without the possibility to both control a stable PIP_2 concentration in the membrane and perform sensitive, time-resolved mass and thickness measurements denied by previously available *in vitro* assays.

MATERIALS AND METHODS

1-Acyl-2-acyl-*sn*-glycero-3-phosphocholine (POPC), L-α-phosphatidylinositol-4,5-bisphosphate (brain, porcine triammonium salt)(PIP_2), and 1-palmytoyl-2-oleoyl-*sn*-glycero-L-serine (POPS) were used. All lipids were purchased from Avanti Polar Lipids, dissolved in chloroform, and stored at −20 °C. All water used in sample cleaning and buffer preparations was Milli-Q grade (Millipore). TBS pH 7.4 buffer was prepared from Milli-Q water with 10 mM Tris(hydroxymethyl)aminomethane (Sigma-Aldrich) and 150 mM NaCl (VWR BDH Prolabo); the pH was adjusted to 7.4 by adding 2 M HCl (Sigma-Aldrich).

Lipid vesicles of the mixtures 7% PIP_2 (POPC/PIP_2 [93:7]), 3.5% PIP_2 (POPC/PIP_2 [96.5:3.5]), and 0.7% PIP_2 (POPC/PIP_2 [99.3:0.7]) and 25% PS (POPC/PS [75:25]) molar ratio were used for this study. All experiments were carried out in TBS pH 7.4. The lipids were mixed to the desired composition in $CHCl_3$. After evaporation of the $CHCl_3$ under constant N_2 flow for 1 h, the lipid film was rehydrated with 1 mL of TBS pH 7.4 to a final lipid concentration of 0.5 mg/mL. After redispersion in TBS pH 7.4 at room temperature, the lipid mixture was sonicated for ∼20 min in a sonication bath (*ULTRA*sonik 104H, NEY) until the solution was clear. The vesicle size was measured by dynamic light scattering at 90° (Zetasizer NanoZS, Malvern Instruments Ltd., U.K.) and analyzed by the Malvern Instrument Software. The measured *Z*-averages for the sonicated vesicles were 110.12 ± 22.7 nm (PDI = 0.193 ± 0.11). The 50 nm vesicles used in the tethering experiment were extruded 31 times through two polycarbonate membranes (pore size 50 nm, Avestin, Canada), and the *Z*-averages obtained by dynamic light scattering at 90° were 55.08 ± 0.91 nm (PDI = 0.289 ± 0.030).

PH-PLCδ_1 Expression in *E. coli*. The PH-PLCδ_1 used in this study was obtained from rat PLCδ_1 (corresponding residues 11-140). A pET11a expression vector carrying the according gene sequence was kindly supplied by Mark Lemmon, Department of Biochemistry and Biophysics, University of Pennsylvania, School of Medicine, Philadelphia, PA. The plasmid was transformed into *Escherichia coli* BL21 (DE3) cells, plated on Luria−Bertani agar containing 100 μg/mL ampicillin, and incubated at room temperature (RT). Single colonies were picked, and three precultures (DYT medium containing 100 μg/mL ampicillin and 1% D-(+)-glucose) were inoculated and incubated overnight at 25 °C (140 rpm). The next morning, six 1.5 L liquid cultures (DYT medium containing 100 μg/mL ampicillin and 1% glucose) were each inoculated with 32 mL of the overnight cultures and were grown at 25 °C (120 rpm). Expression was induced by adding isopropyl-β-D-thiogalactopyranoside (IPTG) to a final concentration of 1 mM at an OD(600) of 0.7. After cell lysis with a high-pressure homogenizer (EmulsiFlex-C5, Avestin, Canada), the peptide was purified first by using an anionic exchange column (QA 52 (Whatman, England), MOPS buffer pH 7, 1 mM EDTA) followed by elution over an ionic strength gradient (buffer A 10 mM MOPS, 1 mM EDTA, pH 7; buffer B 10 mM MOPS, 500 mM NaCl, 1 mM EDTA, pH 7). The peptide was further subjected to a cationic exchange column (CM 52, Whatman, England), and finally small impurities (DNA fragments) were removed by gel filtration and elution in phosphate buffer (100 mM $NaPO_4$, 150 mM NaCl, pH 7). Fractions were pooled and stored at −80 °C. The mass spectra and the sequence analysis of the purified peptide can be found in the Supporting Information.

Bilayer Formation on the DPI Waveguide and Protein Domain Adsorption. Dual polarization interferometry was used to monitor supported lipid bilayer formation and to study the binding of PH-PLCδ_1 to PIP_2 containing SLBs.[11,12] DPI allows measurement of changes in the refractive index and optical thickness at high resolution caused by molecular film deposition within the evanescent field on the waveguide surface through recording in real time the phase shift of two different linear polarizations of light coupled through the waveguide.[11] For optically anisotropic films, such as supported lipid bilayers, a known optical film thickness can be used instead to calculate changes in the refractive index (proportional to mass) and birefringence (related to ordering of the lipids) from the phase shift changes recorded by the DPI instrument.[13] The adsorbed lipid mass and layer birefringence was calculated using this method assuming 4.7 nm thickness for the SLB and a specific refractive index (dn/dc) of 0.135 for the lipid bilayer.[13] All calculations were performed after linear baseline correction for instrumental drift. The thickness of the SLB with the adsorbed PH-PLCδ_1 peptide was also modeled as 4.7 nm since the actual peptide coverage was less than 20%, which is the approximate limit for which a correct thickness increase is obtained through DPI.[14] A dn/dc of 0.182[15] was used for the PH-PLCδ_1 to calculate the adsorbed peptide mass.

DPI experiments were performed at 20 °C (see the Supporting Information for comparison to 37 °C) on an Analight BIO200 (Farfield Group Ltd., United Kingdom) instrument. A dual slab waveguide sensor chip (22 mm × 6 mm) with a silicon oxide surface was used for all DPI experiments. DPI waveguides were sonicated in acetone for 30 min, then in EtOH for 30 min, dried with filtered nitrogen, and then exposed to UV−ozone for 40 min before usage. The waveguides were sonicated in between experiments in 2% SDS for 20 min, rinsed with Milli-Q water, sonicated in ethanol for 20 min, dried with filtered nitrogen, and exposed to UV−ozone for 30 min. Lipid vesicles of the desired lipid composition were injected to form a SLB on the DPI waveguide by the method pioneered by McConnell et al. and described by Mashaghi et al. for its use in the DPI.[13,16] The incubation times were chosen based on quartz crystal microbalance with dissipation monitoring (QCM-D) and fluorescence

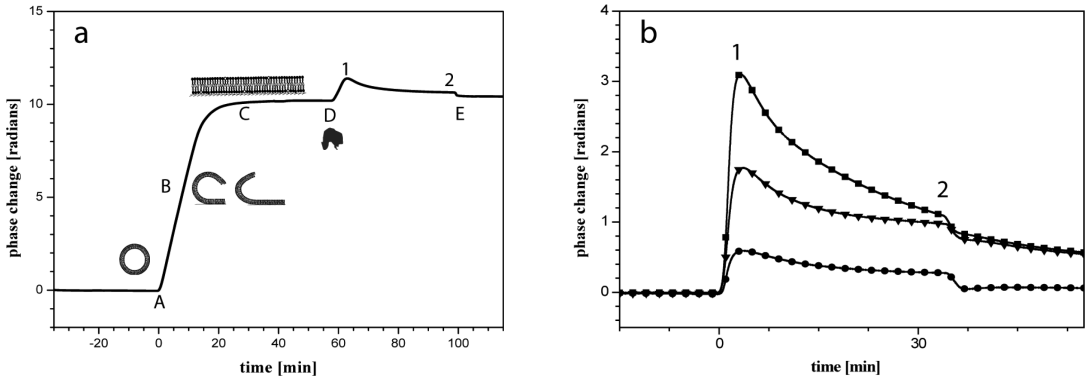

Figure 1. (a) Typical time evolution for SLB formation followed by peptide exposure in a DPI experiment. PIP_2 lipid vesicle solution (7%) is injected (A), and the vesicles adsorb to the silicon oxide chip surface (B) and start to rupture and fuse to form a SLB (C). After rinsing with buffer, the 2 μM PH-PLCδ_1 is injected (D) over 34 min at a constant flow (5 μL/min). At the end of the peptide adsorption (E), buffer is injected again. Analysis of the PH-PLCδ_1 mass adsorption was done at the peak value (1) and before the buffer rinse (2). (b) Adsorption of 2 μM PH-PLCδ_1 on 0.7%, 3.5%, and 7% PIP_2 SLBs. ■, 7% PIP_2 (POPC/PIP_2 [90:10]); ▼, 3.5% PIP_2 (POPC/PIP_2 [95:5]); ●, 0.7% PIP_2 (POPC/PIP_2 [99:1]). PH-PLCδ_1 (2 μM in TBS pH 7.4) was injected with 5 μL/min for 34 min onto the SLB surface. For PIP_2 containing SLBs, a pronounced peak adsorption of PH-PLCδ_1 was observed shortly after injection (time point 1) with a gradual decrease to a plateau value (time point 2).

Table 1. PH-PLCδ_1 Adsorption at Increasing Concentration on 7% PIP_2 Containing POPC SLBs[a]

PH-PLCδ_1 [μM]	m_{max} [ng/cm^2]	adsorption peak (1) [ng/cm^2]	adsorption plateau (2) [ng/cm^2]	adsorption after rinse (E) [ng/cm^2]	$K_{a(2)}$ [$\times 10^5$ M^{-1}]
0.5	172.2	14.4 ± 2.7	11.2 ± 0.6	9.9 ± 0. 5	1.4 ± 0.1
1	172.2	31.4 ± 7.2	22.9 ± 4.3	18.1 ± 1.4	1.5 ± 0.3
2	172.2	82.0 ± 1.9	27.1 ± 9.5	16.2 ± 3.2	0.9 ± 0.4

[a] The adsorbed mass on the lipid bilayer increases with rising peptide concentration. The adsorption peak corresponds to time point 1, adsorption plateau corresponds to time point 2, and the value after rinsing corresponds to time point E in Figure 1. The calculated maximal mass, m_{max}, is based on the assumption of a 1:1 binding of PH-PLCδ_1 to the PIP_2 head group (a monolayer of PH-PCLδ_1 would be 208.7 ng/cm^2 assuming hexagonal close-packing). Affinity constants are calculated for the plateau values (n = 3).

recovery after photo bleaching (FRAP) microscopy experiments.[10] In total, 500 μL of lipid vesicles solution (100 μg/mL lipid concentration in TBS, pH 7.4) was used to load the injection loop (capacity 200 μL). A volume of 170 μL of the vesicle solution was injected at 50 μL/min flow rate, and the flow stopped for 30 min during which a SLB was formed. Excess liposomes were rinsed with 200 μL of TBS (pH 7.4) at 50 μL/min flow rate after which the flow rate was reduced to 5 μL/min. After reestablishment of a constant baseline for the SLB (typically less than 0.01 radians drift/30 min), 170 μL of the PH-PLCδ_1 was injected at a flow of 5 μL/min (yielding a 34 min exposure of the SLB to the peptide solution). The bilayer was subsequently rinsed at 5 μL/min with TBS (pH 7.4). The control experiments with DNA-tethered liposomes were performed using the Membrane Protein Analysis Kit from Layerlab (Layerlab AB, Göteborg, Sweden) according to an adaptation of the manufacturer's instructions (Layerlab AB, Göteborg, Sweden).[17] After the baseline was recorded in TBS, the NeutrAvidin/biotin-ssDNA solution was injected. The NeutrAvidin moiety was allowed to adsorb electrostatically to the waveguide surface for 30 min and subsequently rinsed. Extruded 50 nm POPC vesicles with 10% PIP_2 incorporated were tethered onto the NeutrAvidin/biotin-ssDNA layer on the DPI waveguide via complementary ssDNA strands.

■ RESULTS

Figure 1a shows the typical time evolution of the TE phase shift in radians (corresponding to molecule adsorption on the chip) upon injection of the vesicle solution and subsequent exposure of the resulting SLB to peptide. A baseline is recorded after chip calibration. At time point A, injection of the lipid vesicles starts and an increase in radians is observed due to the adsorbed mass on the SiO_2 chip surface. The maximum of adsorbed lipid vesicles to a substrate surface, as can be determined from the dissipation shift with QCM-D,[18] coincides with the maximum in birefringence observed by DPI.[13] After this maximum vesicle density, which will depend on, e.g., the lipid composition,[19] temperature,[20] substrate,[20b,21] and buffer conditions,[19a,20b,21] has been reached on the chip surface (time point B), the vesicles start to rupture and fuse to form a planar lipid bilayer (time point C).[13,18] At time point C, stable mass and birefringence values are obtained, where the birefringence has been shown to depend on, e.g., the lipid composition, buffer ion composition, and lipid phase.[13] Excess lipid material is removed by subsequent rinsing. The adsorbed mass of lipids per square centimeter was calculated[13] as a control for SLB formation and found to be 4.41 ± 0.46 (ng/mm^2) for 7% PIP_2, 4.98 ± 0.56 (ng/mm^2) for 3.5% PIP_2, 4.14 ± 0.66 (ng/mm^2) for 0.7% PIP_2, and 4.94 ± 0.29 (ng/mm^2) for POPC using $(dn/dc)_{lipid}$ = 0.135 (cm^3/g) and an assumed SLB thickness of 4.7 nm. The supported lipid bilayer birefringence (BF_{SLB}) was calculated assuming this thickness to determine the quality of the formed SLBs in each experiment with the method described by Mashaghi et al.[13] The average birefringence of the data set was BF_{SLB} = 0.0149 ± 0.0055, which together with the obtained mass values are in good agreement with the formation of

dx.doi.org/10.1021/ac2009178 |Anal. Chem. 2011, 83, 6267–6274

Table 2. Affinity Constants for 2 μM PH-PCLδ_1 Adsorbed on SLB with Increasing PIP_2 Content[a]

% PIP_2 in SLB	m_{max} [ng/cm^2]	adsorption peak (1) [ng/cm^2]	adsorption plateau (2) [ng/cm^2]	adsorption after rinse (E) [ng/cm^2]	$K_{a(2)}$ [$\times 10^5$ M^{-1}]
0.7	17.2	16.8 ± 1.7	7.4 ± 0.7	2.1 ± 0.8	3.7 ± 0.6
3.5	86.1	52.0 ± 4.0	22.8 ± 4.5	10.0 ± 6.1	1.8 ± 0.5
7	172.1	82.0 ± 1.9	27.1 ± 9.5	16.2 ± 3.2	0.9 ± 0.4

[a] The constant was calculated using the plateau value (time point 2 in Figure 1) and assuming hexagonal close packing of the SLB (n = 3).

SLBs, as the mass values for a layer of vesicles of similar size is at least 50% higher and the birefringence 2−3 times higher. Such data was discarded and attributed to aging of waveguides through deterioration from use and cleaning, and a new waveguide was chosen.

Characterization of the quality and lipid mobility of the PIP_2 containing SLBs produced with the same protocols by complementary techniques (QCM-D and FRAP) has previously been described in detail in ref 22, revealing that SLBs with few defects could be generated under the conditions used in this study on silicon oxide surfaces. This study also revealed that the mobile fraction of PIP_2 lipids decreases as their membrane fraction increases.[22]

Influence of peptide bulk concentration on the adsorption was tested on 7% PIP_2 in POPC SLBs. The PIP_2 concentration was selected to be high for ease and reliability of detection and for presenting enough binding sites for formation of a dense peptide layer while still being in the physiologically relevant range of PIP_2 in membranes.[23] Adsorption was tested with 0.5, 1, and 2 μM PH-PLCδ_1. Figure 1B shows the time evolution of PH-PLCδ_1 adsorption onto PIP_2 containing SLBs (■ corresponds to 7% PIP_2). After injection (D, Figure 1a) the adsorption reaches a maximum (1, Figure 1a,b) followed by a gradual decrease to a plateau value (2, Figure 1a,b) before buffer rinsing (E, Figure 1a). This behavior was found at all investigated concentrations for SLBs containing PIP_2. When PH-PLCδ_1 instead was injected to a POPC SLB as control, a peak was never observed and the additional mass associated with the surface and measured by DPI was within the error margin of the measurement the same after the initial adsorption and before rinsing. As expected, the adsorbed mass increased with increasing PH-PLCδ_1 concentration (see Table 1). Affinity constants were calculated for the plateau values (2) using the Langmuir isotherm model and assuming a maximal hexagonal close packing of the PH-PCLδ_1 with an average diameter of 30 Å for the PH-PCLδ_1 (Table 1 in the Supporting Information for detailed information on the parameters used).[24] The calculated affinity constants are based on the assumption of full accessibility and optimal distribution of half of the PIP_2 lipid binding sites in the lipid bilayer (one leaflet) on the time scale of the experiments. We point out that a lower number of accessible binding sites, e.g., through steric blocking of neighboring or nondiffusing PIP_2 at a high concentration of PIP_2 or through asymmetric distribution of PIP_2 between the lipid leaflets will lead to an underestimated K_a with our model assumptions.

POPC SLBs containing 0.7%, 3.5%, and 7% of PIP_2 were assembled on the DPI sensor chips to assess the influence of PIP_2 concentration in SLBs on 2 μM PH-PLCδ_1 membrane adsorption. The PH-PLCδ_1 domain was injected (D, Figure 1a) into the flow chamber to interact with the SLB surface. Figure 1b shows the time evolution of 2 μM PH-PLCδ_1 adsorption onto three different bilayer compositions (●, 0.7% PIP_2; ▼, 3.5% PIP_2; and ■, 7% PIP_2). With increasing PIP_2 content in the SLB, higher

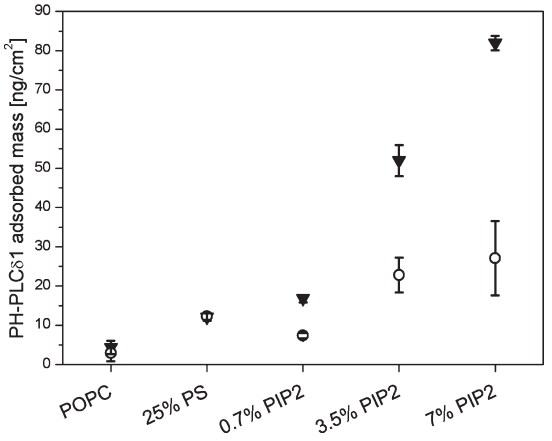

Figure 2. PH-PLCδ_1 (2 μM) adsorbed on bilayers mimicking different surface charge densities. ▼ corresponds to the peak in adsorption (time point 1 in Figure 1) and ○ corresponds to the plateau values in adsorption before rinsing (time point 2 in Figure 1). Higher mass adsorption of the peptide was measured with increasing PIP_2 lipid concentration in the POPC SLB. SLBs with 25 mol % PS have the same surface charge as 7 mol % PIP_2 SLBs but show much lower PH-PLCδ_1 adsorption. For PIP_2 containing membranes, a significantly higher initial (peak) adsorption of PH-PLCδ_1 is observed relative to the equilibration (plateau) value (n = 3). Note, the symbols for the "peak" on the non-PIP_2 containing membranes are only shown as a guide and are the same within the drift as in the corresponding reported plateau values.

adsorbed peptide mass was detected for the same peptide concentration. With increasing PIP_2 content in the bilayer, also the initial adsorbed mass of the peptide increased and the subsequent decrease was more pronounced (see Table 2). Affinity constants were again calculated for the plateau values (2) using the Langmuir isotherm model and the same assumptions as described above (Table 2). For the highest concentrations of 7% PIP2 and 2 μM PH-PLCδ_1, the adsorption just equilibrated before the sample was consumed, leading to a higher variance in this data point as some measurements were not fully equilibrated.

We considered the possibility that adsorption of PH-PLCδ_1 to a PIP_2 containing supported lipid bilayer can be explained by nonspecific electrostatic interactions, since the high negative charge of PIP_2 is likely to attract the positively charged loops of the PH-PLCδ_1. PS, which carries a net charge of −1 at pH 7.4,[25] is widely distributed within many cellular membranes and is used as a negatively charged lipid to mimic the composition of inner plasma membranes.[26] It has been reported to bind nonspecifically to many types of membrane associated proteins.[26c,27] SLBs are doped with 25% PS to obtain a similar average membrane surface charge as 7% PIP_2 containing SLBs were formed to investigate the degree of specificity of the adsorption. (−3.5 negative charges per PIP_2 molecules were assumed in pH 7.4, and 25% PS were incorporated into POPC lipid vesicles to

mimic the same surface charge as calculated for 7% PIP_2 vesicles.[23,27a]) The distribution of both negatively charged lipids (PIP_2 and PS) between the SLB leaflets is not thought to be strongly affected by the negative surface potential of the silicon oxide substrate as Rossetti et al. have shown by FRAP experiments for PS on SiO_2,[28] probably as a consequence of strong screening in the high ionic strength buffer. A much lower peptide adsorption was found on the PS containing SLBs (initial (peak) value after adsorption, 12.1 ± 1.0 ng/cm^2; plateau, 12.2 ± 1.0 ng/cm^2) compared to on 7% PIP_2 containing SLBs (peak, 82.0 ± 1.9 ng/cm^2; plateau, 27.1 ± 9.5 ng/cm^2). Although the adsorption was higher than on the pure POPC control (initial (peak) value after adsorption, 4.4 ± 1.7 ng/cm^2; plateau, 2.9 ± 2.1 ng/cm^2, Figure 2), the values were closer to 0.7% PIP_2, which indicates only weak electrostatic association of the PH-PLCδ_1 with the negatively charged SLB surface. Importantly, in addition to the difference in affinity (equilibrium adsorbed amount of peptide), we also observed qualitatively different adsorption kinetics for the stronger binding to PIP_2 than for the weaker binding to PS. The adsorption on bilayers incorporating PIP_2 goes through a pronounced initial peak in adsorbed mass (triangles, Figure 2), which after desorption reaches a plateau value (circles, Figure 2). In contrast, this pronounced peak is missing and the initial and final adsorbed masses are similar for bilayers lacking PIP_2. Note, the symbols for the "peak" for the POPC and PS membranes are only shown as a guide. For these membranes, no peak was observed for the peptide adsorption, so the given values correspond to the mass values after saturated adsorption, which within system drift correspond to the reported plateau values.

Control experiments with DNA-tethered liposomes were performed to assess if the mass decrease after the initial peak value is the result of a change in the optical properties of the SLB after PH-PLCδ_1 adsorption, as this can affect the response of the DPI. A possible scenario for the apparent mass loss after the initial adsorption of PH-PLCδ_1 onto PIP_2 containing SLBs is that peptide insertion into the membrane expands the membrane but lowers the mass density of the SLB plus peptide in the sensing region. Such membrane expansion outside the sensing region is not possible if the adsorption experiment is performed on tethered liposomes. The vesicle membranes are closed. That is, on scales larger than the 100 nm size of the liposomes, no lateral exchange of material can occur within the surface-tethered membranes. Thus adsorption of peptide to a vesicle can somewhat increase the liposome size, but the liposome with all its material will remain within the laterally defined sensing zone of the waveguide. The SLB extends outside the lateral confines of the sensing zone due to the design of the chip and the instrument measurement cell and can expand as more material is inserted. Therefore a similar behavior observed for tethered liposomes will imply actual (peptide) mass loss from the membrane, as lateral expansion and thinning can be ruled out. Control experiments with adsorption of 2 μM PH-PLCδ_1 on 7% PIP_2 tethered vesicles gave peak values of 83.0 ± 3.1 ng/cm^2 and plateau values of 24.2 ± 5.5 ng/cm^2 (see the Supporting Information, SI Figure 3) and thus very similar kinetics compared to the adsorption of the peptide to 7% PIP_2 SLBs. Furthermore, repeated injections of the PH-PLCδ_1 to the same SLB led to an insignificant reduction in the amount of equilibrium bound peptide for subsequent adsorptions (see the Supporting Information , SI Figure 4). If the peptide removed PIP_2 from the membrane, a continuous reduction in the number of PIP_2 binding sites with time is expected and adsorption for a subsequent injection would be reduced by the number of lost binding sites from the first injection, which corresponds to the number of reversible binding events. We observe an increase in the total binding, including the irreversibly bound peptide fraction, which can be explained by a de facto increase of binding sites after PIP_2 translocation from the bottom leaflet between injections to compensate for blocked binding sites by irreversibly bound peptide.[29] This indicates a similar number of accessible PIP_2 binding sites in the SLB and thus demonstrates that PH-PLCδ_1 binding and rinsing did not remove PIP_2 from the SLB.

DISCUSSION

Dual polarization interferometry is an excellent technique for assessing bilayer quality and therefore granting the same conditions for all peptide adsorption experiments. The error bars obtained for the mass of SLBs incorporating PIP_2 compared to pure POPC SLBs indicate some variability from partial SLB formation when PIP_2 is mixed in. Peptide adsorption on partially formed SLBs leads to irreproducible results and can also lead to different kinetics. Therefore evaluation of the SLBs before peptide adsorption by calculating the adsorbed mass proved to be vital since complete SLBs were not formed at all times.

DPI allowed for studying the kinetics of the peptide binding to the SLB in high detail. In addition to binding specificity and affinity constants, important information on the kinetics of peptide binding was obtained. Without detection of the adsorption peak and later the displacement of the peptide, an incomplete picture would result. Affinity constants determined with techniques that are not sensitive enough to detect these variations might therefore not truly describe the nature of such versatile interaction partners as proteins and lipids and in the worst case result in incorrect quantification from assuming incorrect equilibrium adsorbed mass. However, the affinity constants calculated from our data using the Langmuir model (Tables 1 and 2) are close to those obtained for whole PLCδ_1 binding to large unilamellar vesicles (LUV) with 2% PIP_2 incorporated ($K_a = 4 \pm 2 \times 10^5$ M^{-1}, Hummel Dreyer filtration technique, and centrifugation assay with sucrose loaded LUVs) by Rebecchi et al. and similar to the K_d of PH-PLCδ_1 and PIP_2 ($K_d = 1.7$ μM measured gives $K_a = 0.6 \times 10^5$ M^{-1}) obtained by isothermal titration calorimetry (ITC) by Lemmon et al.[8,26c] Our measurements demonstrated a clear decrease in the affinity constant with increasing PIP_2 concentration in the SLBs. This trend toward lower affinity constants for higher incorporated PIP_2 in the SLBs can also be observed by comparing the two literature values for 2% PIP_2 and 5% PIP_2 (obtained with different techniques) reported above.

The difference observed in DPI measurements between the adsorbed peak and plateau masses increases with increasing PIP_2 concentration in the SLBs. Two tentative explanations for this behavior can be formulated. First, with an increasing amount of PIP_2 in the SLBs, the difference increases between adsorbed mass (plateau value) and the maximum calculated possible surface coverage. Assuming PH-PLCδ_1 domain clusters in solution, larger spacing between the PIP_2 head groups for the lower incorporated fractions would allow for aggregated peptides being adsorbed to the SLB whereas with higher PIP_2 in the SLB these peptides would to a larger extent be expelled due to steric repulsion. The possibility of binding of peptide multimers to the PIP_2 containing SLB is further discussed in the analysis of the detailed binding kinetics.

Table 3. Birefringence (BF) Values for Different Adsorption Models[a]

% PIP_2 in SLB	$BF_{PH\text{-}PLC\delta_1}$	$BF_{SLB+PH\text{-}PLC\delta_1} - BF_{SLB}$
0.7	-0.0001 ± 0.0002	0.0005 ± 0.0004
3.5	-0.0010 ± 0.0008	0.0020 ± 0.0010
7	-0.0007 ± 0.0002	0.0035 ± 0.0023

[a] The adsorption of the PH-PLCδ_1 was modeled assuming an adlayer of 3 nm (approximate diameter of PH-PLCδ_1 from the crystal structure[24]) for the protein domain ($BF_{PH\text{-}PLC\delta_1}$) and once neglecting the contribution to the layer thickness from the PH domain ($BF_{SLB+PH\text{-}PLC\delta_1} - BF_{SLB}$) using the same overall layer thickness of 4.7 nm (as for the SLB).

The second possible scenario would be PIP_2 sequestering during binding of the PH-PLCδ_1 to the SLB surface. Although no clustering has been reported for PH-PLCδ_1 adsorption and no ordered domain formation of PIP_2 was found in membranes,[23,30] the preferred location of some PIP_2 in the vicinity of the adsorbed peptide could mask them for interaction with PH-PLCδ_1 and thus depress the calculated affinity constants, since the maximum number of binding sites would not be correctly estimated. Furthermore a high fraction of immobile PIP_2 has been observed in SLBs.[10] With an increasing PIP_2 fraction, it is statistically more likely that an immobile PIP_2 would be in the vicinity of an already occupied PIP_2 binding site and thus more likely to be entirely blocked or close enough to lead to steric repulsion of coadsorbed aggregated PH-PLCδ_1.

In either case, the apparent K_a would decrease with increasing PIP_2 content and the observation should lead to caution about the interpretation of affinity constants obtained when single-reaction processes might not be observed or when a mixture of mobile and immobile binding sites might be present. We stress that this is likely to be true also in native systems.

The observed unusual adsorption kinetics, i.e., the peak in PH-PLCδ_1 mass adsorption, is almost exclusively observed for specific interactions with PIP_2 containing SLBs. Although also observed in a fraction of measurements on the bare waveguides, it is not observed on control supported lipid bilayer preparations without PIP_2 and the observed peak is orders of magnitudes higher on PIP_2 than on the strongly negatively charged bare waveguides. Thus, although a maximum is therefore not exclusively observed for specific interaction it is clear that among our membrane systems only the specifically interacting PIP_2 membranes display this kinetics and that the specific interaction with PIP_2 strongly induces this behavior.

Possible scenarios to explain this behavior could be the loss of PIP_2 lipids from the SLB over the time of the adsorption, insertion of the peptide into the SLB, or initial clustering of the peptides and subsequent displacement of unbound peptides. Loss of PIP_2 from the SLB was ruled out by repeated injections of the PH-PLCδ_1, which led to renewed adsorption of similar amounts of peptide as the initial injection after correcting for an irreversibly bound fraction of peptide. This demonstrates insignificant loss of binding sites, which leads us to conclude that the amount of PIP_2 in the SLB stayed the same also after peptide desorption. Insertion of the PH-PLCδ_1 into the SLB, causing bilayer spreading, was also rejected by the controls using DNA-tethered vesicles, for which the same adsorption kinetics was observed as for an SLB of the same composition. The most probable explanation for the observed kinetics is therefore actual mass loss due to desorption of weakly bound peptide. It is possible that the PH-PLCδ_1 clusters in bulk solution are due to the mostly conserved strong dipolar electrostatic polarization of PH domains that supports a general function in binding to phospholipid membranes.[31] After initial weak electrostatic association with the membrane, loosely bound peptide is expelled upon stronger specific binding of the PH-PLCδ_1 to the PIP_2 head groups. The same dissociation or rearrangement might explain the similar but much weaker behavior during the adsorption of the peptide to the bare waveguide, although on a much smaller scale, as the peptide is electrostatically reorienting on the surface and expelling weakly associated peptides.

The irreversibly binding peptide fraction, which was present in all experiments and shown to increase with multiple injections and increased peptide concentration, also has several possible causes. In addition to denaturation producing a higher affinity, e.g., for the hydrophobic core of the membrane, our proposed model for explaining the presence of the adsorption peak could also help explain the presence of an irreversibly bound peptide fraction. Some peptide aggregates could also remain at the membrane surface and bind multivalently to the PIP_2 membrane. This will results in a significantly higher effective binding affinity, approximating irreversible binding.

DPI can be used to in detail probe the layer structure of adsorbed biomolecule films and in particular reorientation of optically anisotropic molecules such as lipids in a well-defined layer.[13] It can thus be used to compare whether PH-PLCδ_1 penetrates into the SLB, if loss of PIP_2 from the SLB occurs, which both should lead to changes in the SLB structure (change in optical birefringence), or if the peptide is likely to adsorb on top of the SLB as predicted for the desorption of excess peptide from the surface as described in the scenario above (change in optical thickness). Modeling of the DPI data and analysis of the obtained birefringence (BF) values (Table 3) indicates that adsorbed PH-PLCδ_1 mainly resides on top of the membrane. The birefringence was first calculated for the SLB in each experiment ($BF_{SLB} = 0.0149 \pm 0.0055$) with the method described by Mashaghi et al.[13] The modeling of the PH-PLCδ_1 adsorption was performed in two different ways. First, it was assumed that the peptide adsorbed as a 3 nm thick adlayer (approximated PH-PLCδ_1 dimension from crystal structure[24]) on top of the SLB with the SLB unperturbed by the binding. The obtained birefringence values ($BF_{PH\text{-}PLC\delta_1}$, Table 3, column 1), are in the range of -1×10^{-3}. A peptide layer can be assumed to be isotropic, and the slightly negative values thus indicate that either the thickness of the layer was overestimated, which could be due to low coverage (only ~20%) of the peptide with respect to the uniform peptide layer assumed by the model, or that the peptide binding causes an effective reduction in alignment of the lipids orthogonal to the waveguide substrate and corresponding decrease in birefringence.[13]

In the second approach, assuming that the PH-PLCδ_1 inserts into the SLB leads to a model where a total layer thickness of 4.7 nm, as used for the SLB calculations, is fixed and the birefringence calculated. The obtained value was used to calculate the change ($BF_{SLB+PH\text{-}PLC\delta_1} - BF_{SLB}$) in birefringence relative to the original SLB, which increased with increasing PIP_2 concentration in the SLB from 0.5×10^{-3} to 3.5×10^{-3} (Table 3, column 2). Since insertion of an optically isotropic peptide, which is shorter than the membrane thickness, should lower the birefringence, a concentration dependent increase is best interpreted as an artifact from underestimation of the true layer thickness. Finally assuming that an optically isotropic peptide layer is adsorbed on top of the 7% PIP_2, SLB yields an

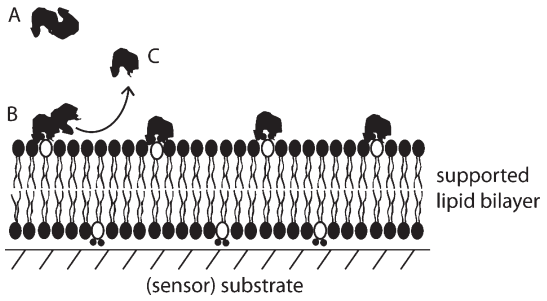

Figure 3. Scheme of PH-PLCδ_1 interaction with the SLB incorporating PIP_2 (outlined lipids). Peptides form clusters in bulk solution (A). Initial electrostatic attraction binds the peptide clusters to the SLB (B) surface. Specific binding to the PIP_2 headgroup breaks the clusters, and nonspecifically associated peptides are expelled from the interface (C).

effective thickness of the peptide of 1.40 ± 0.22 nm in the layer with supposedly low peptide density (plateau value).

With comparison of these modeling results, an isotropic peptide layer on top of the SLB with a slight distortion of the lipid alignment or density seems to fit best, as a combination of the first and last approaches suggest. A significant amount of lipid loss from the SLB by PIP_2 removal through desorbing PH-PLCδ_1 would have led also to a large reduction in birefringence as lipids in the SLB assume a more disordered alignment due to the lower density. Thus, also the birefringence analysis supports the adsorption of peptides on top of the SLB followed by desorption of only a weakly adsorbed peptide as the plausible interpretation of the unusual binding kinetics (Figure 3). On the basis of the accumulated data, we propose as our model for the adsorption process that after an initial electrostatic attraction to the SLB surface the PH-PLCδ_1 binds specifically to PIP_2, breaking up clusters and expelling nonspecifically associated peptide from the surface. The weaker, nonspecific, electrostatic interaction to PS-containing membranes is not sufficient to cause this expulsion. However, it should be noted that specificity might not be required to initiate this behavior. A sufficiently strong attraction of the positively charged binding domain to orient it to the surface might be enough, as a weak peak, interpreted as the expulsion of excess aggregated peptide, is also observed on the bare waveguides.

The peak in adsorption can be influenced by initial electrostatic attraction of the peptide to the negatively charged SLB surface. Adsorption of the PH-PLCδ_1 on 25% PS containing SLBs resulted in less adsorbed mass than on 7% PIP_2 containing SLB displaying the same surface charge density. However, the local surface charge density around a PIP_2 headgroup is several times higher than around a PS headgroup. The observed difference in the bound amount is well in agreement with the documented specific binding of PH-PLCδ_1 to the PIP_2 headgroup and association only by electrostatic attraction of the PH-PLCδ_1 with the 25% PS SLBs.[8,26c] The difference observed in the adsorption kinetics with no pronounced change in adsorbed mass for 25% PS SLBs in contrast to high initial adsorption with subsequent mass loss for 7% PIP_2 also agrees with initial electrostatic attraction and later specific adsorption to the PIP_2 headgroup on the 7% PIP_2 SLBs and only electrostatic association of the peptide on the PS SLBs (see Figure 2).

CONCLUSIONS

Using DPI to monitor SLB formation and peptide adsorption allowed measuring both the affinity and time-resolved kinetics of protein domain binding to a lipid headgroup. A novel analysis of SLB birefringence changes in response to interaction between peptides and the SLB also resulted in a best fit assuming a model where PH-PLCδ_1 adsorbs on top of the SLB, adding conformational information on the interaction. A decrease was observed for the affinity constants calculated from the peptide mass adsorbed at equilibrium for increasing fractions of PIP_2 in the SLBs. This may indicate a more complex interaction between peptide clusters and lipids in the membrane, which could mean that affinity constants calculated based on a simple one-rate affinity constant analysis as the Langmuir model are not fully appropriate to describe the interaction. Monitoring the detailed time evolution of the adsorption led to detection of multiple binding steps and allowed selection of an optimal time point for affinity analysis of the adsorption. The obtained affinity constants scale with both PIP_2 and peptide concentration as previously reported for the system.[8,26c] Control measurements with SLBs of a similar surface charge but no specific interaction allowed linking the three-phase adsorption process to strong interaction, as exemplified by specific interaction, of the PH-PLCδ_1 to PIP_2. Desorption of clustered peptide seems plausible from the new type of kinetic analysis using SLBs, although despite reports documenting no clustering of PIP_2 in membranes[23,30a,c] and no cluster formation of PIP_2 upon interaction with PH-PLCδ_1,[30b] multivalent binding of the peptide to the surface cannot be conclusively excluded. We emphasize that with this platform also other proteins can be similarly studied in a stable environment for their interaction with a specific lipid headgroup and a differentiated view on the adsorption behavior over time can be gained.

ASSOCIATED CONTENT

Supporting Information. Additional information as noted in text. This material is available free of charge via the Internet at http://pubs.acs.org.

AUTHOR INFORMATION

Corresponding Author
*E-mail: erik.reimhult@boku.ac.at.

ACKNOWLEDGMENT

The authors thank Prof. Mark Lemmon for kindly providing the vectors for PH-PLCδ_1 expression and Helene Fäh-Rechsteiner and Prof. Rudi Glockshuber for lab resources, experimental expertise, help in protein expression, and purification. We gratefully acknowledge the EU-FP7-NMP-ASMENA and Swiss National Science Foundation, NCCR Project "Nanoscale Science" for research funding.

REFERENCES

(1) Lemmon, M. A. *Nat. Rev. Mol. Cell. Biol.* **2008**, *9*, 99–111.
(2) (a) Cremona, O.; De Camilli, P. Phosphoinositides in membrane traffic at the synapse *J. Cell Sci.* **2001**, *114*, 1041–1052. (b) Gilmore, A. P.; Burridge, K. Regulation of vinculin binding to talin and actin by phosphatidyl-inositol-4-5-bisphosphate *Nature* **1996**, *381*, 531–535. (c) Hilgemann, D. W.; Feng, S.; Nasuhoglu, C. The Complex and Intriguing Lives of PIP2 with Ion Channels and Transporters. *Sci. STKE* **2001**, *2001*, re19, DOI: 10.1126/stke.2001.111.re19. (d) Janmey, P. A.; Lindberg, U. Cytoskeletal regulation: rich in lipids *Nat. Rev. Mol. Cell. Biol.* **2004**, *5*, 658–666.

(3) (a) James, S. R.; Paterson, A.; Harden, T. K.; Demel, R. A.; Downes, C. P. *Biochemistry* **1997**, *36*, 848–855. (b) Laux, T.; Fukami, K.; Thelen, M.; Golub, T.; Frey, D.; Caroni, P. *J. Cell Biol.* **2000**, *149*, 1455–1472. (c) Pike, L. J.; Miller, J. M. *J. Biol. Chem.* **1998**, *273*, 22298–22304. (d) Tran, D.; Gascard, P.; Berthon, B.; Fukami, K.; Takenawa, T.; Giraud, F.; Claret, M. *Cell. Signalling* **1993**, *5*, 565–581. (e) Wu, D.; Huang, C. K.; Jiang, H. *J. Cell Sci.* **2000**, *113*, 2935–2940.

(4) Tyers, M; Haslam, R. J.; Rachubinski, R. A.; Harley, C. B. *J. Cell. Biochem.* **1989**, *40*, 133–145.

(5) Rebecchi, M. J.; Scarlata, S. *Annu. Rev. Biophys. Biomol. Struct.* **1998**, *27*, 503–528.

(6) (a) Blomberg, N.; Baraldi, E.; Sattler, M.; Saraste, M.; Nilges, M. *Structure* **2000**, *8*, 1079–1087. (b) Lemmon, M. A.; Ferguson, K. M. *Biochem. J.* **2000**, *350*, 1–18. (c) Lietzke, S. E.; Bose, S.; Cronin, T.; Klarlund, J.; Chawla, A.; Czech, M. P.; Lambright, D. G. *Mol. Cell* **2000**, *6*, 385–394. (d) Worthylake, D. K.; Rossman, K. L.; Sondek, J. *Nature* **2000**, *408*, 682–688.

(7) Lemmon, M. A.; Ferguson, K. M.; Abrams, C. S. *FEBS Lett.* **2002**, *513*, 71–76.

(8) Lemmon, M. A.; Ferguson, K. M.; O'Brien, R.; Sigler, P. B.; Schlessinger, J. *Proc. Natl. Acad. Sci. U.S.A.* **1995**, *92*, 10472–10476.

(9) (a) Garcia, P.; Gupta, R.; Shah, S.; Morris, A. J.; Rudge, S. A.; Scarlata, S.; Petrova, V.; McLaughlin, S.; Rebecchi, M. J. *Biochemistry* **1995**, *34*, 16228–16234. (b) Kavran, J. M.; Klein, D. E.; Lee, A.; Falasca, M.; Isakoff, S. J.; Skolnik, E. Y.; Lemmon, M. A. *J. Biol. Chem.* **1998**, *273*, 30497–30508. (c) Szentpetery, Z.; Balla, A.; Kim, Y.; Lemmon, M.; Balla, T. *BMC Cell Biol.* **2009**, *10*, 67. (d) Yagisawa, H.; Hirata, M.; Kanematsu, T.; Watanabe, Y.; Ozaki, S.; Sakuma, K.; Tanaka, H.; Yabuta, N.; Kamata, H.; Hirata, H. *J. Biol. Chem.* **1994**, *269*, 20179–20188.

(10) Baumann, M.; Amstad, E.; Mashaghi, A.; Reimhult, E.; Textor, M. *Biointerphases* **2010**submitted.

(11) Swann, M. J.; Peel, L. L.; Carrington, S.; Freeman, N. J. *Anal. Biochem.* **2004**, *329*, 190–198.

(12) Cross, G. H.; Reeves, A. A.; Brand, S.; Popplewell, J. F.; Peel, L. L.; Swann, M. J.; Freeman, N. J. *Biosens. Bioelectron.* **2003**, *19*, 383–390.

(13) Mashaghi, A.; Swann, M.; Popplewell, J.; Textor, M.; Reimhult, E. *Anal. Chem.* **2008**, *80*, 3666–3676.

(14) Cross, G. H.; Freeman, N. J. Dual Polarization Interferometry: A Real-Time Optical Technique for Measuring (Bio)Molecular Orientation, Structure and Function at the Solid/Liquid Interface; In *Handbook of Biosensors and Biochips*; John Wiley & Sons: Oxford, 2008.

(15) Vörös, J. *Biophys. J.* **2004**, *87*, 553–561.

(16) (a) McConnell, H. M.; Watts, T. H.; Weis, R. M.; Brian, A. A. *Biochim. Biophys. Acta : Rev. Biomembranes* **1986**, *864*, 95–106. (b) Terry, C. J.; Popplewell, J. F.; Swann, M. J.; Freeman, N. J.; Fernig, D. G. *Biosens. Bioelectron.* **2006**, *22*, 627–632.

(17) G. Layerlab AB, Sweden, www.layerlab.se, Instructions for Users (Biacore), Membrane Protein Analysis Kit.

(18) Reimhult, E.; Zäch, M.; Höök, F.; Kasemo, B. *Langmuir* **2006**, *22*, 3313–3319.

(19) (a) Richter, R. P.; Berat, R.; Brisson, A. R. *Langmuir* **2006**, *22*, 3497–3505. (b) Merz, C.; Knoll, W.; Textor, M.; Reimhult, E. *Biointerphases* **2008**, *3*, FA41–FA50.

(20) (a) Reimhult, E.; Hook, F.; Kasemo, B. *Phys. Rev. E* **2002**, 66. (b) Reimhult, E.; Hook, F.; Kasemo, B. *Langmuir* **2003**, *19*, 1681–1691.

(21) Kumar, K.; Tang, C. S.; Rossetti, F. F.; Textor, M.; Keller, B.; Voros, J.; Reimhult, E. *Lab Chip* **2009**, *9*, 718–725.

(22) Baumann, M. K.; Amstad, E.; Mashaghi, A.; Textor, M.; Reimhult, E. *Biointerphases* **2010**, *5*, 114–119.

(23) Herrig, A.; Janke, M.; Austermann, J.; Gerke, V.; Janshoff, A.; Steinem, C. *Biochemistry* **2006**, *45*, 13025–13034.

(24) Lomize, M. A.; Lomize, A. L.; Pogozheva, I. D.; Mosberg, H. I. *Bioinformatics* **2006**, *22*, 623–625.

(25) Toner, M.; Vaio, G.; McLaughlin, A.; McLaughlin, S. *Biochemistry* **1988**, *27*, 7435–7443.

(26) (a) Carvalho, K.; Ramos, L.; Roy, C.; Picart, C. *Biophys. J.* **2008**, *95*, 4348–4360. (b) Gambhir, A.; Hangyas-Mihalyne, G.; Zaitseva, I.; Cafiso, D. S.; Wang, J.; Murray, D.; Pentyala, S. N.; Smith, S. O.; McLaughlin, S. *Biophys. J.* **2004**, *86*, 2188–2207. (c) Rebecchi, M.; Peterson, A.; McLaughlin, S. *Biochemistry* **1992**, *31*, 12742–12747. (d) Hokanson, D. E.; Ostap, E. M. *Proc. Natl. Acad. Sci. U.S.A.* **2006**, *103*, 3118–3123.

(27) (a) McLaughlin, S.; Wang, J.; Gambhir, A.; Murray, D. *Annu. Rev. Biophys. Biomol. Struct.* **2002**, *31*, 151–175. (b) Solon, J.; Gareil, O.; Bassereau, P.; Gaudin, Y. *J. Gen. Virol.* **2005**, *86*, 3357–3363.

(28) Rossetti, F. F.; Textor, M.; Reviakine, I. *Langmuir* **2006**, *22*, 3467–3473.

(29) Reimhult, E.; Kasemo, B.; Hook, F. *Int. J. Mol. Sci.* **2009**, *10*, 1683–1696.

(30) (a) Fernandes, F.; Loura, L. M. S.; Fedorov, A.; Prieto, M. *J. Lipid Res.* **2006**, *47*, 1521–1525. (b) Gokhale, N. A.; Abraham, A.; Digman, M. A.; Gratton, E.; Cho, W. *J. Biol. Chem.* **2005**, *280*, 42831–42840. (c) van Rheenen, J.; Mulugeta Achame, E.; Janssen, H.; Calafat, J.; Jalink, K. *EMBO J.* **2005**, *24*, 1664–1673.

(31) (a) Blomberg, N.; Baraldi, E.; Nilges, M.; Saraste, M. The PH superfold: a structural scaffold for multiple functions *Trends Biochem. Sci.* **1999**, *24*, 441–445. (b) DiNitto, J. P.; Cronin, T. C.; Lambright, D. G. Membrane Recognition and Targeting by Lipid-Binding Domains. *Sci. STKE* **2003**, *2003*, re16, DOI: 10.1126/stke.2132003re16.